Available online at www.sciencedirect.com
ScienceDirect
Geomorphology 87 (2007) 284–301
GEOMORPHOLOGY
www.elsevier.com/locate/geomorph

Cosmogenic nuclide measurements in southernmost South America and implications for landscape change

M.R. Kaplan [a,*], A. Coronato [b], N.R.J. Hulton [a], J.O. Rabassa [b], P.W. Kubik [c], S.P.H.T. Freeman [d]

[a] School of GeoSciences, University of Edinburgh, Edinburgh, EH8 9XP, Scotland, UK
[b] Laboratorio de Geología del Cuaternario, CADIC-CONICET, Ushuaia 9410, Tierra del Fuego, Argentina
[c] Paul Scherrer Institut, c/o Institute of Particle Physics, HPK H30, ETH Hoenggerberg, CH-8093 Zurich, Switzerland
[d] Scottish Universities Environmental Research Centre, East Kilbride G75 0QF, UK

Received 7 September 2005; received in revised form 28 September 2006; accepted 1 October 2006
Available online 28 November 2006

Abstract

We measured in situ ^{10}Be, ^{26}Al and ^{36}Cl on glacial deposits as old as 1.1 Myr in the southernmost part of Patagonia and on northern Tierra del Fuego to understand boulder and moraine and, by inference, landscape changes. Nuclide concentrations indicate that surface boulders have been exposed for far less time than the ages of moraines they sit upon. The moraine ages are themselves constrained by previously obtained ^{40}Ar/^{39}Ar ages on interbedded lava flows or U-series and amino acid measurements on related (non-glacial) marine deposits. We suggest that a combination of boulder erosion and their exhumation from the moraine matrix could cause the erratics to have a large age variance and often short exposure histories, despite the fact that some moraine landforms are demonstrably 1 Myr old. We hypothesize that fast or episodic rates of landscape change occurred during glacial times or near the sea during interglacials. Comparison with boulder erosion rates and exhumation histories derived for the middle latitudes of semi-arid Patagonia imply different geomorphic processes operating in southernmost South America. We infer a faster rate of landscape degradation towards the higher latitudes where conditions have been colder and wetter.

Keywords: Cosmogenic; Geomorphology; Quaternary; Glacial geology; South America; Argentina

1. Introduction

Surface exposure measurements using in situ cosmogenic nuclides in southern South America allow study of the timing and rates of Earth surface processes well beyond the limits of the radiocarbon method. We investigated the exposure history of boulders on moraines older than the last glacial maximum (LGM, ~25 to 17 ka; Kaplan et al., 2004; McCulloch et al., 2005) in the southernmost part of Patagonia and on northern Tierra del Fuego. Our investigation indicates that in these areas cosmogenic nuclide data from erratics located on glacial drift deposits cannot be used reliably to constrain glacial chronologies of landforms older than ~25 ka. This finding differs from that in central Patagonia (Kaplan et al., 2005), despite the semi-arid climate and preservation of original morphology in the area (Ercolano et al., 2004), but is similar to other studies on 'old'

* Corresponding author. Present address: Geochemistry, LDEO, Columbia University, Palisades, NY 10964, USA. Tel.: +1 8453658652.
E-mail address: mkaplan@ldeo.ed.ac.uk (M.R. Kaplan).

0169-555X/$ - see front matter © 2006 Elsevier B.V. All rights reserved.
doi:10.1016/j.geomorph.2006.10.005

moraines (cf., Putkonen and O'Neal, 2006). On the other hand, the data provide quasi-quantitative information on the rates of moraine degradation, boulder exhumation and erosion, and thus geomorphic processes in this region. Such knowledge has potentially a wide range of implications, from understanding South American landscape development to offshore studies of the products of continental erosion.

2. Regional setting and prior chronology

Southern South America has the longest, most complete record of Quaternary glaciations in the world outside Antarctica (Mercer, 1983; Clapperton, 1993; Coronato et al., 2004a; Rabassa et al., 2005). Figs. 1 and 2 show the boundaries of former glaciations in Patagonia and Tierra del Fuego, including the maximum extent of

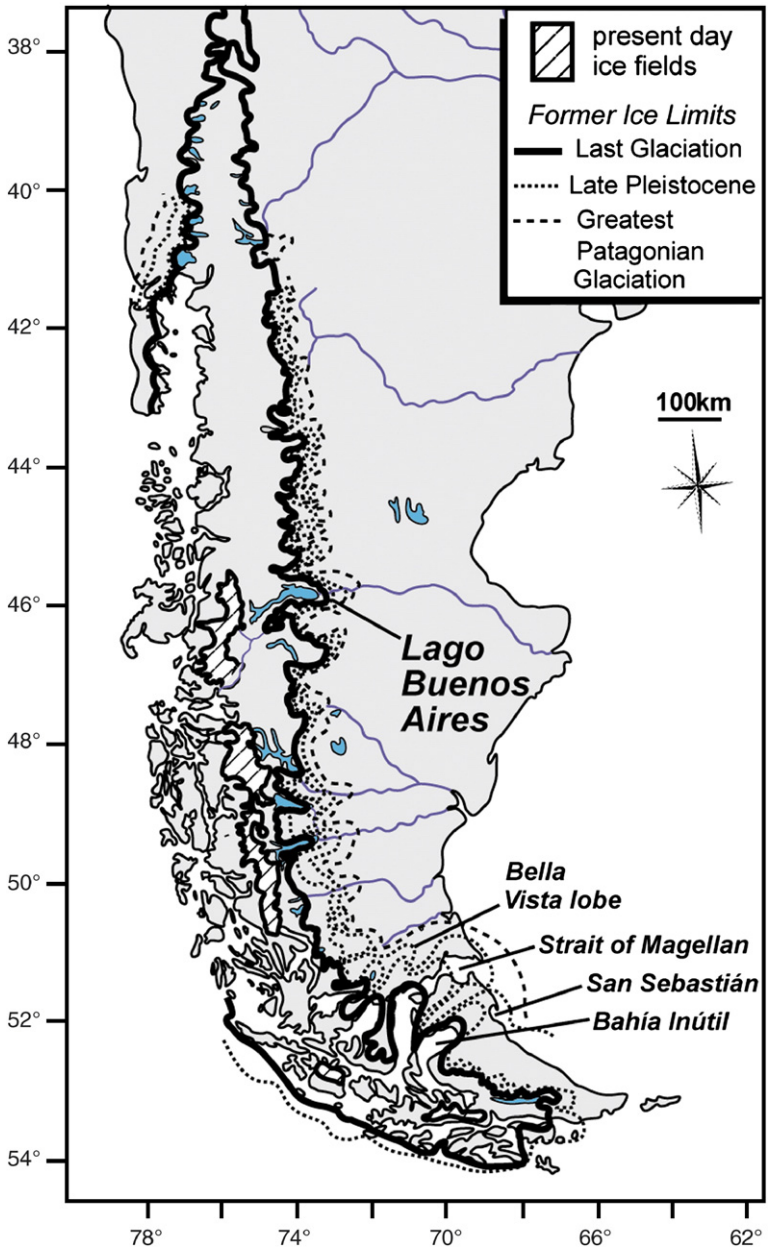

Fig. 1. Simplified from Singer et al. (2004) and based on original work of Caldenius (1932). Map of southern South America showing major areas mentioned in the text and outline of Quaternary glaciations. The locations of the three former ice lobes discussed throughout the text are indicated (Table 1).

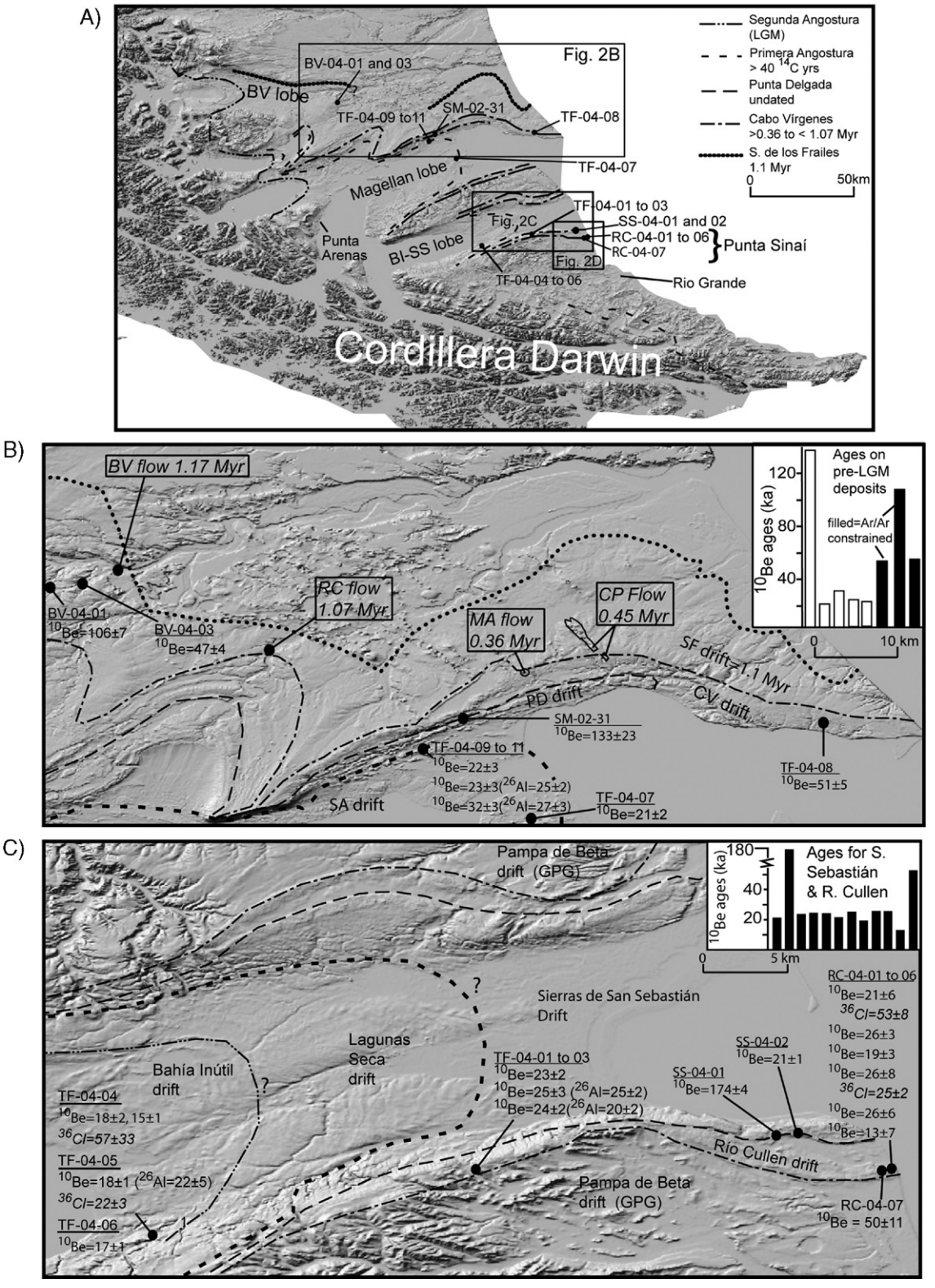
A)
Segunda Angostura (LGM)
Primera Angostura > 40 14C yrs
Punta Delgada undated
Cabo Vírgenes >0.36 to < 1.07 Myr
S. de los Frailes 1.1 Myr
0
50km
Fig. 2B
BV-04-01 and 03
BV lobe
TF-04-09 to11
SM-02-31
TF-04-08
TF-04-07
Magellan lobe
Fig. 2C
TF-04-01 to 03
SS-04-01 and 02
RC-04-01 to 06
RC-04-07
Punta Sinaí
Fig. 2D
Punta Arenas
BI-SS lobe
TF-04-04 to 06
Rio Grande
Cordillera Darwin
B)
BV flow 1.17 Myr
RC flow 1.07 Myr
MA flow 0.36 Myr
CP Flow 0.45 Myr
BV-04-01 10Be=106±7
BV-04-03 10Be=47±4
SF drift ~1.1 Myr
PD drift
CV drift
SM-02-31 10Be=133±23
TF-04-09 to 11 10Be=22±3 10Be=23±3(26Al=25±2) 10Be=32±3(26Al=27±3)
TF-04-07 10Be=21±2
TF-04-08 10Be=51±5
SA drift
Ages on pre-LGM deposits
filled=Ar/Ar constrained
10Be ages (ka)
120
80
40
0
10 km
C)
Pampa de Beta drift (GPG)
Ages for S. Sebastián & R. Cullen
10Be ages (ka)
180
40
20
0
5 km
Sierras de San Sebastián Drift
Lagunas Seca drift
Bahía Inútil drift
TF-04-04 10Be=18±2, 15±1 36Cl=57±33
TF-04-05 10Be=18±1 (26Al=22±5) 36Cl=22±3
TF-04-06 10Be=17±1
TF-04-01 to 03 10Be=23±2 10Be=25±3 (26Al=25±2) 10Be=24±2(26Al=20±2)
SS-04-01 10Be=174±4
SS-04-02 10Be=21±1
RC-04-01 to 06 10Be=21±6 36Cl=53±8 10Be=26±3 10Be=19±3 10Be=26±8 36Cl=25±2 10Be=26±6 10Be=13±7
Río Cullen drift
Pampa de Beta drift (GPG)
RC-04-07 10Be = 50±11

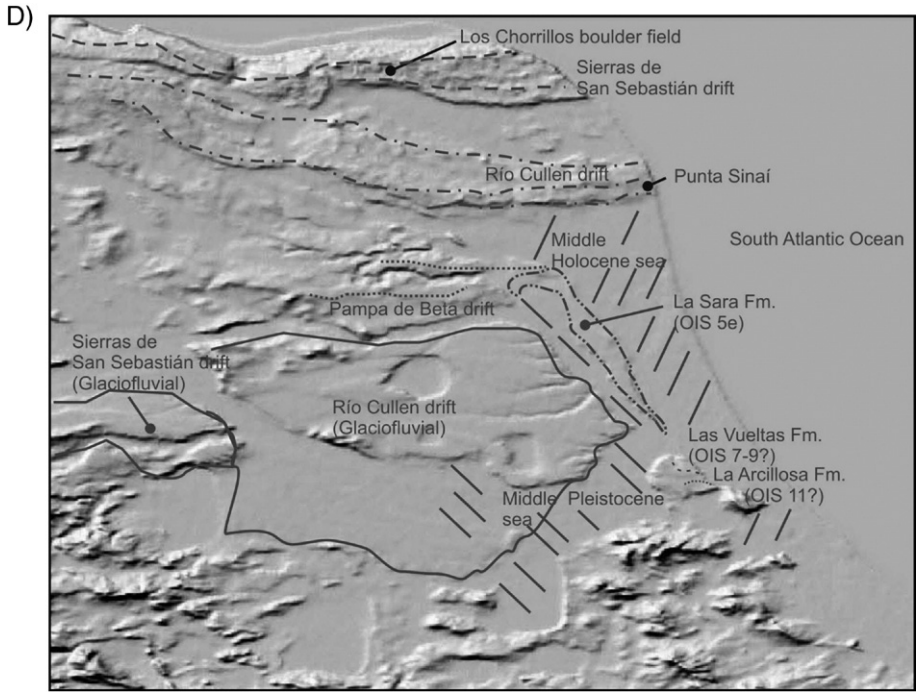

Fig. 2. Maps of Fuego–Southernmost Patagonia with major glacial limits (Meglioli, 1992; Rabassa et al., 2000; Bentley et al., 2005), locations of all samples measured in this study, and locations of independent age constraints, given on Shuttle Radar Topography Mission (STRM) 3 arc sec shaded relief elevation data (http://gisdata.usgs.net/Website/Seamless/). A. Overview of three former ice lobes and 5 major glacial units correlated across the area. The names of the units are for the Magellan lobe (see Table 1). Area of B, C, and D outlined. B. Detailed map of north side of outer Magellan Strait showing limits of glacial drifts and age data. Also shown in inset is histogram of ages. Samples from moraines constrained in age with limiting $^{40}Ar/^{39}Ar$ dated lava flows have filled bars. BV = Bella Vista; RC = Rio Ciaike; MA = Monte Aymond; CP = Cerro la Pirca; SA = Segunda Angostura; PD = Punta Delgada; CV = Cabo Vírgenes; and SF = Sierra de Los Frailes. C. Detailed map showing details of glacial limits and age data obtained on Tierra del Fuego. Inset shows ages for the Sierras de San Sebastián and Río Cullen drifts— note that the age *Y*-scale changes and there are two ages >50 ka. D. Focus on the Bahía Inútil–San Sebastián ancient ice lobe, its associated drift units, and related interglacial materials (see text). The boulder field near Punta Sinaí with ^{10}Be dates (Fig. 2C) is located in the hummocky Río Cullen moraine, at present forming an active sea-cliff on its eastern edge. Southwestward of Punta Sinaí the two glaciofluvial fans (solid outline) were formed by paraglacial (e.g., glaciofluvial) processes during the Río Cullen and San Sebastián glaciations, which provided gravels for the later marine depositional processes. The area was occupied by the sea during MIS 11, 7–9 and 5e interglacials and the Middle Holocene, forming – from the present coast to inland – gravel ridges, beaches and estuarine environments. During MIS 5e the best preserved marine raised terrace (La Sara Fm.) was deposited (after Meglioli, 1992; Coronato et al., 1999; Bujalesky et al., 2001).

former ice, the Greatest Patagonian Glaciation (GPG). Interbedded lava flows and glacial deposits have allowed application of $^{40}Ar/^{39}Ar$, K-Ar and cosmogenic dating techniques, which provide, or at least constrain, the ages of the different glacial units and events that have occurred in southern South America over the Late Tertiary and Quaternary Periods (Mercer, 1983; Singer et al., 1997, 2004; Kaplan et al., 2005). The focus of this investigation is the glacial record in Fuego–southernmost Patagonia.

Three former ice lobes existed in southernmost Patagonia/northern Tierra del Fuego, which are discussed throughout this paper. From north to south, these are the Rio Gallegos, Magallen and Bahía Inútil–San Sebastián ice lobes (Fig. 2; Table 1). Five distinct glacigenic (stratigraphic) deposits are associated with each of the three lobes, which were defined by Meglioli (1992) who built upon the work of Caldenius (1932). Mapping presented here (Table 1; Fig. 2) is based on their work. Meglioli (1992) and others (e.g., Rabassa et al., 2000; Coronato et al., 2004b) correlated the five different glacial deposits based on a suite of relative weathering indexes and chronological constraints. These include relationship of outwash deposits to moraines, moraine morphology, physical characteristics of the till (color, oxidation, depth of weathering, grussfication of clasts, weathering of pebbles), till boulder frequency and weathering, cryogenic features (presence and size of frost wedge casts), soil thickness, and logical reconstruction of ice lobe geometry (oldest extents have little or no obvious relation to frontal topography). The major glaciations represented by the five

units are 'nested' within each other (Fig. 2), the younger ones at inner and/or lower positions in the landscape. The chronology used to constrain the age of the deposits includes radioisotopic dates on interbedded lava flows, and amino acid racimization (AAR), U-series, and infinite radiocarbon dates on fossil material in marine sediments morpho-stratigraphically related to the drift units.

The oldest glacial drift is associated with the GPG, which is well-constrained in age in the area studied (Mercer, 1983; Meglioli, 1992; Ton-That et al., 1999; Rabassa et al., 2000; Singer et al., 2004). $^{40}Ar/^{39}Ar$ ages of 1168±14 and 1070±20 (Fig. 2B; Bella Vista (BV) and Río Cullen (RC) flows) on basalts above and below the Bella Vista drift (which was deposited by the Rio Gallegos *lobe* during the GPG) provide maximum and minimum ages, respectively (Meglioli, 1992; Singer et al., 2004). Singer et al. (2004) provided an additional minimum $^{40}Ar/^{39}Ar$ age of 1016±14 ka on a lava flow overlying GPG drift at Lago Buenos Aires (LBA) ~1000 km to the north (Fig. 1), indicating an age of the GPG of ~1.1 Myr considering all the sites. Other local minimum ages for the GPG drift are provided (Meglioli, 1992) by three dated basalt flows, at 320±20, 310±30, 360±40, and 450±100 ka, which stratigraphically overlie the Sierra de Los Frailes Drift, the GPG equivalent for the Magellen lobe (i.e., a correlative to the Bella Vista drift of the Rio Gallegos lobe, Table 1); the two 'oldest minimum' $^{40}Ar/^{39}A$ ages for the GPG Sierra de Los Frailes Drift, on the Monte Aymond (MA) and Cerro la Pirca (CP) lava flows, are shown on Fig. 2B.

The first major drift unit younger than GPG drift in Fuego–southernmost Patagonia includes the Cabo Vírgenes drift for the Magellan lobe (and its correlatives; Table 1). This drift is also constrained in age with minimum $^{40}Ar/^{39}Ar$ ages of 450±100 and 360±40 ka on the Monte Aymond and Cerro la Pirca lava flows (Fig. 2) north of the Strait of Magellan (Meglioli, 1992). The next two younger drift units, e.g., the Punta Delgada and Primera Angostura drifts for the Magellan lobe, are only indirectly dated with two ^{14}C ages of 47 and 45 ^{14}C ka BP in shelly till just north of Punta Arenas. These radiocarbon dates are assumed to be infinite and therefore minimum ages for these two drift units and the glaciations they represent (Porter, 1990; Clapperton et al., 1995). AAR data also strongly support a pre-LGM age for the Primera Angostura and, thus, older moraine material (Meglioli, 1992; Clapperton et al., 1995; McCulloch et al., 2005). In addition, a suite of relative dating methods, including soil development and weathering rind thickness, and topographic setting, suggest that at least a glacial cycle separates the Primera Angostura (and equivalents) from the younger Segunda Angostura glacial record deposited during marine oxygen isotope stage (MIS) 2 (Porter, 1990; Meglioli, 1992). Based on the ^{14}C, AAR, topographic setting, and relative weathering data the Primera Angostura has been assumed to be 150 ka (i.e., MIS 6) and the Punta Delgada drift at least one glacial cycle older (e.g., Rabassa et al., 2000). The youngest major drift unit in Fuego–southernmost Patagonia, e.g., Segunda Angostura Drift in the Magellan area, corresponds to the LGM, ca. 25 to 17.6 ka (Clapperton et al., 1995; Sugden, 2005; McCulloch et al., 2005; Kaplan et al., in preparation).

The deposits and ages described above were for the Rio Gallegos and Strait of Magellan lobes. South of the Magellan Straits, the third lobe of interest, the Bahía Inútil–San Sebastián lobe, deposited four major drift units on both sides of this depression; namely, from older to younger, Río Cullen, San Sebastián, Lagunas Secas and Bahía Inútil drifts. All these units are morainic systems and younger than the GPG, represented locally by the Pampa de Beta Drift, which is preserved only as till remnants on the higher tablelands (Meglioli, 1992; Rabassa et al., 2000; Coronato et al., 2004b). Areas focused on in this study include near Punta Sinaí and Chorrillos, which are on the Río Cullen and San Sebastián drifts (Fig. 2D), respectively. Given the lack of lava flows south of the Strait of Magellan there are no $^{40}Ar/^{39}Ar$ age constraints on these drifts. However, age constraints on the glacial deposits are provided by AAR and U-series data on (interglacial) raised marine terraces and geomorphological analysis of glaciofluvial fans, as suggested by Bujalesky et al. (2001), in addition to the correlations between the three lobes described above. The Río Cullen Drift is considered to be younger than the GPG (ca. 1 Ma) and older than an interglacial marine terrace dated at ca. 400–600 ka (U-series on marine shells). The San Sebastián Drift is assumed to be >300 ka and <400–600 ka, based also on U-series ages of the related interglacial marine terraces. During the last interglacial, a marine terrace composed of La Sara Formation (Fig 2C), of identified Sangamon age (MIS 5e; Codignoto and Malumian, 1981; Rutter et al., 1989; Bujalesky et al., 2001), developed when the sea eroded the margins of the Río Cullen and San Sebastián moraines and extensive marine beaches were deposited south of Punta Sinaí. The two other, younger drifts (Lagunas Secas and Bahía Inútil Drifts) are found much farther west of the Punta Sinaí area and away from the interglacial terraces. They are correlated with the penultimate and last glaciations, respectively (Rabassa et al., 2000; McCulloch et al., 2005).

Table 1
Correlation of glacial deposits on Tierra del Fuego and southernmost Patagonia discussed in the paper

Rio Gallegos lobe	Strait of Magellan lobe	Bahía Inútil–San Sebastián lobe	Chronology based on the following	Reference	Cosmo ages this paper (ka)
Seno Almirante Montt Drift	**Segunda Angostura Drift**	**Bahía Inútil Drift**	25 to ~ 12 ka; ^{14}C and ^{10}Be dates	1–4	15–18
Rio Turbio Drift	Primera Angostura Drift	Lagunas Secas Drift	>40 ^{14}C yrs and pre-LGM AAR data	1–3	32–21
Not recognized	*Punta Delgada Drift*	Sierras de San Sebastián Drift	U-series ages and pre-LGM AAR data	1–3	174, 21, 133
Glencross Drift	**Cabo Vírgenes Drift**	*Río Cullen Drift*	>0.36 to <1.07 Myr, U-series and AAR data	1, 3	50–13
Bella Vista Drift	Sierra de los Frailes Drift	*Pampa de Beta Drift*	1.1 million years, ^{40}Ar/^{39}Ar	1, 3, 5	106 and 47

In bold, drift units constrained by ^{40}Ar/^{39}Ar dated interbedded lava flows (Fig. 2) or ^{14}C and cosmogenic ages. In *italics*, other drift units, which are constrained in age by infinite ^{14}C ages, amino acid or U series data, or correlation to the dated drift units (see text). References for chronology in the column to the left: 1, Meglioli, 1992; 2, Clapperton et al., 1995; 3, Rabassa et al., 2000; 4, McCulloch et al., 2005; 5, Singer et al., 2004.

To summarize, across Fuego–southernmost Patagonia five different units, for three different lobes, shown in Table 1 and on Fig. 2, have been correlated to each other based on a suite of techniques and dates. These include, for example, position from the mountains, relation to topography (e.g., post Cabo Vírgenes there were 'distinct' ice lobes along easternmost area), relative weathering features, absolute ages on interbedded lava flows, and infinite ^{14}C, AAR, and U-series data on shells from related interglacial or marine sediments.

3. Sampling and methods

Sampling for surface exposure measurements was targeted at moraine crests or drift units older than the LGM (Table 2). A multi-nuclide approach allowed 'checks' on the different isotopic chronometers, specifically ^{10}Be which is used mainly. All the erratics sampled were quartzites, granites or granodiorites originating from within the Andes. ^{10}Be concentrations were measured on a quartzite and granite sample (BV-04-01 and 03) from two different moraine crests on the Bella Vista drift, deposited by the Río Gallegos ice lobe (Fig. 2). ^{10}Be was measured on one erratic from the Cabo Vírgenes Drift (TF-04-08), and ^{10}Be, ^{36}Cl and ^{26}Al on ten erratics from the equivalent Río Cullen drift (RC-04-01 to -07 and TF-04-01 to -03) associated with the adjacent ice lobe, including seven samples from near Punta Sinaí (Fig. 2A). The Punta Sinaí samples are all granodiorites (D. Acevedo, personal communication). Two samples were collected from the San Sierras de San Sebastián Drift; one sample was measured from Punta Delgada drift (SM-02-31); and four from the younger Primera Angostura drift (TF-04-07, TF-04-09 to -11). ^{10}Be, ^{36}Cl, and ^{26}Al were also measured in three erratics from a kame terrace just southeast of Bahía Inútil (TF-04-04 to -06), which we assumed from field evidence to be part of pre-LGM Laguna Seca drift (Bentley et al., 2005).

We preferentially selected the largest boulders available on moraine crests. Samples were collected with hammer and chisel from the upper few cm of moraine boulders, at least 5 cm from edges and sharp facets. Elevations were recorded using a GPS; based on comparisons (when possible) to elevations recorded with a barometric-based altimeter standardized to sea level, GPS elevation accuracy is estimated to be within 10–20 m. Snow cover is not corrected for, but it is assumed to have had an insignificant effect on ages (<1%; presently, mean annual precipitation < 500 mm with no appreciable snow accumulation) at least during interglacial times.

For ^{10}Be and ^{26}Al, quartz was separated and purified at the University of Edinburgh following the method outlined in Bierman et al. (2002) and Ivy-Ochs (1996). ^{10}Be/Be and ^{26}Al/Al isotope ratios were measured at the AMS facility in Zurich operated jointly by the Paul Scherrer Institut and ETH Zurich, or the Scottish Universities Environmental Research Centre (Tables 3 and 4).

For ^{36}Cl analyses, the four measurements in Table 2 are on the same erratics as for the ^{10}Be and ^{26}Al analyses. Initial processing was at the University of Edinburgh and the samples were prepared so that the measurement was done on either the quartz or quartz–feldspar fraction (Table 6). The pure quartz sample (TF-04-04), which was measured to try to isolate the neutron activation pathway (cf., Liu et al., 1994), barely produced a measurement (1σ is >50%), perhaps due to a lack of target ^{35}Cl. Three other quartz-rich samples were also prepared (for RC-04-04, RC-04-03, and TF-04-06), but these produced no measurable ^{36}Cl, and are not presented. The three other samples in Table 2 (TF-04-05, RC-04-01 and

Table 2
Sample location and information

Sample	Lat. °S	Long. °W	Elev (km)	Sample mass (g)	Sample thickness (cm)	Boulder height (cm)	Prod. rate ^{10}Be (atoms/g/yr)	Prod. rate ^{26}Al (atoms/g/yr)	Prod. rate ^{36}Cl (atoms/g/yr)	Drift unit
Río Gallegos lobe										
BV-04-01	51 55.379	70 50.955	0.240	6.574	3.9	240	7.47			Bella Vista
BV-04-03	51 54.319	70 43.807	0.221	13.057	2.0	225	6.78			Bella Vista
Strait of Magellan lobe										
TF-04-07	52 35.315	69 27.404	0.100	37.276	2.6	49	6.00			Primera Angostura
TF-04-08	52 18.200	68 38.616	0.037	36.891	1.0	99	5.72			Cabo Vírgenes
TF-04-09	52 23.124	69 45.672	0.092	12.741	0.5	127	6.06			Primera Angostura
TF-04-10	52 22.808	69 45.252	0.122	21.259	1.5	38	6.19	40.23		Primera Angostura
TF-04-11	52 22.694	69 44.835	0.093	30.742	0.9	78	6.05	39.30		Primera Angostura
SM-02-31	52 17.910	69 42.965	0.179	1.207	1.5	25	7.19			Punta Delgada
Bahía Inútil–San Sebastián lobe										
Southeast of Bahía Inútil										
TF-04-04	53 29.446	69 13.060	0.090	23.908	2.5	300–400	5.95		0.633	Bahía Inútil
TF-04-05	53 29.437	69 13.235	0.090	26.649	1.4	151–300	– –	39.02	2.389	Bahía Inútil
TF-04-06	53 29.606	69 13.100	0.101	24.086	1.0	300–600	6.09			Bahía Inútil
Between Bahía Inútil and San Sebastián										
TF-04-01	53 24.889	68 43.589	0.199	26.169	1.8	150	6.65			Río Cullen
TF-04-02	53 23.711	68 43.703	0.236	26.482	2.1	130	6.87	44.63		Río Cullen
TF-04-03	53 23.733	68 43.912	0.236	31.798	2.4	128	6.85	44.52		Río Cullen
South side of Bahia San Sebastián										
SS-04-01	53 20.480	68 15.678	0.012	22.4616	2.5	480	6.05			S. de Sebastián
SS-04-02	53 20.399	68 13.307	0.07	17.1311	2.5	275	5.83			S. de Sebastián
Near Punta Sinaí										
RC-04-01	53 24.252	68 04.916	0.016	16.121	1.5	300	5.57		1.146	Río Cullen
RC-04-02	53 24.326	68 05.122	0.022	15.579	1.5	150	5.61			Río Cullen
RC-04-03	53 24.426	68 05.165	0.021	16.081	1.5	167	5.60			Río Cullen
RC-04-04	53 24.374	68 05.259	0.023	16.427	2.2	319	5.58		11.63	Río Cullen
RC-04-05	53 24.176	68 05.089	0.017	20.116	1.9	150	5.56			Río Cullen
RC-04-06	53 24.453	68 05.130	0.012	19.856	1.1	75	5.57			Río Cullen
RC-04-07	53 24.631	68 07.279	0.021	14.467	1.2	104	5.61			Río Cullen

Total production rate for ^{36}Cl includes all pathways (see Tables 5 and 6 for composition). All Río Cullen samples are granodiorites. Other samples lithologies not noted individually but were granodiorites, granite, or similar.

TF-04-04f) were mainly quartz, but they did contain some K-bearing grains and these provided measurable ^{36}Cl/Cl (Tables 5 and 6) due to spallation production. Non-quartz grains remained in the two samples TF-04-05 and RC-04-01 because they were not leached long enough in Hydrofluoric/Nitric acids. For TF-04-04f, some feldspar grains were purposely left in the sample to ensure a ^{36}Cl AMS measurement, given the uncertainty of 'pure' quartz having enough target ^{35}Cl. Final preparation of samples for ^{36}Cl/Cl, including dissolution and extraction, followed methods outlined in Stone et al. (1996a) at the Cosmogenic Isotope Laboratory at the University of Washington. Before dissolution, a ~1 g aliquot was taken for ICP analyses (Table 6), and ^{37}Cl added to the remaining sample. ^{36}Cl/^{35}Cl and ^{35}Cl/^{37}Cl were measured at the Center for Accelerator Mass Spectrometry at Lawrence Livermore National Laboratory. Target element concentrations and the neutron production and capture properties of samples analysed for ^{36}Cl are based on XRF analyses of major elements and ICP–MS analyses of trace Gd and Sm (Table 5). B was measured by ICP–OES. U and Th were not measured and were assumed to be 3±1 and 15±3, respectively (Table 5).

For age calculations, we use the ^{10}Be–^{26}Al exposure age calculator at http://hess.ess.washington.edu-/math/al_be_stable/al_be_multiple.php. This program uses a global production rate of 4.98 ± 0.34 atoms/g/yr for ^{10}Be (±2σ; sea level and high latitude and standard atmosphere; Gosse and Stone, 2001). Production by neutron spallation and muons are 4.87±0.33 and 0.11±0.01 atoms/g/yr, respectively. The ^{26}Al production rate used is based on the production ratio ^{26}Al:^{10}Be of 6.5±0.4 (Kubik et al., 1998) with a muogenic component of

Table 3
Concentration and age data for ^{10}Be measurements

Sample	^{10}Be	Age1	Age2	Drift unit
		No erosion (ka)	Erosion (ka)	
Rio Gallegos lobe				
BV-04-01	7.73E+ 05±4.95E+ 04	106±7.0	124±9.7	Bella Vista
BV-04-03	3.18E+ 05±2.89E+ 04	47.4±4.3	50.2±4.9	Bella Vista
Strait of Magellan lobe				
TF-04-07	1.27E+ 05±9.49E+ 03	21.2±1.6	21.8±1.7	Primera Angostura
TF-04-08	2.86E+ 05±2.69E+ 04	50.7±4.8	54.0±5.5	Cabo Vírgenes
TF-04-09	1.30E+ 05±1.62E+ 04	21.6±2.7	22.1±2.8	Primera Angostura
TF-04-10	1.43E+ 05±1.61E+ 04	23.3±2.6	24.0±2.8	Primera Angostura
TF-04-11	1.89E+ 05±2.06E+ 04	31.6±3.4	32.8±3.7	Primera Angostura
SM-02-31	9.30E+ 01±1.58E+ 05	133±23	164±36	Punta Delgada
Bahía Inútil–San Sebastián lobe				
Southeast of Bahía Inútil				
TF-04-04	1.09E+ 05±1.22E+ 04	18.4±2.1	18.9±2.2	Bahía Inútil
TF-04-04*	9.04E+ 04±4.65E+ 03	15.2±0.8	15.5±0.8	Bahía Inútil
TF-04-05*	1.07E+ 05±5.43E+ 03	17.8±0.9	18.2±1.0	Bahía Inútil
TF-04-06*	1.00E+ 05±4.27E+ 03	16.5±0.7	16.9±0.7	Bahía Inútil
Between Bahía Inútil and San Sebastián				
TF-04-01	1.55E+ 05±1.43E+ 04	23.4±2.2	24.1±2.3	Río Cullen
TF-04-02	1.70E+ 05±2.01E+ 04	24.9±2.9	25.6±3.1	Río Cullen
TF-04-03	1.67E+ 05±1.03E+ 04	24.5±1.5	25.2±1.6	Río Cullen
South side of Bahia San Sebastián				
SS-04-01*	1.01E+ 06±2.12E+ 04	174±3.8	232±7.1	S. de Sebastián
SS-04-02*	1.22E+ 05±5.23E+ 03	21.1±0.9	21.6±1.0	S. de Sebastián
Near Punta Sinaí				
RC-04-01	1.18E+ 05±3.29E+ 04	21.4±5.9	21.9±6.3	Río Cullen
RC-04-02	1.45E+ 05±1.65E+ 04	26.1±3.0	26.9±3.2	Río Cullen
RC-04-03	1.07E+ 05±1.41E+ 04	19.2±2.5	19.7±2.7	Río Cullen
RC-04-04	1.45E+ 05±4.47E+ 04	26.2±8.1	27.0±8.6	Río Cullen
RC-04-05	1.44E+ 05±3.30E+ 04	26.1±6.0	27.0±6.4	Río Cullen
RC-04-06	7.31E+ 04±3.86E+ 04	13.2±7.0	13.4±7.2	Río Cullen
RC-04-07	2.75E+ 05±5.80E+ 04	49.6±10	52.7±12	Río Cullen

All ages calculated using ^{10}Be–^{26}Al exposure age calculator (http://hess.ess.washington.edu-/math/al_be_stable/al_be_multiple.php). All measurements carried out at ETH except those with asterisk, which were performed at SUERC (TF-06-04 measured twice). Age2 calculated with an erosion rate of 1.4 mm/kyr (see text). A weighted mean used of the following procedural blanks (10^{-14} with % error): 1.21 (23.5), 3.72 (31.8), 1.80 (32.8), 1.76 (23.8), 1.67 (37.3) and for SUERC measurements 3.870E− 15 (22.9) and 5.2064E− 15 (25.8).

0.022% at sea level (Stone, 2000). Production rates for all cosmogenic nuclides are corrected for a local air pressure of 1002 mbar and annual temperature of 281 K at sea level (Taljaard et al., 1969; Gosse and Stone, 2001). For ages >100 ka (only ^{10}Be was measured on samples exposed for this length of time), we increase the spallation production rate by 11% given the evidence for a higher long-term rate in southern Patagonia (Ackert et al., 2003), although we emphasize that using the different production rate decreases the ages by ~10% and has no effect on our interpretations and main conclusions. ^{36}Cl production rates are calculated using sea-level, high latitude values of 48.8 and 4.8 atoms/gCa/yr from spallation and muon capture reactions on Ca respectively, and 161 and 10.2 atoms/gK/yr from spallation and muon capture reactions on K respectively (Stone et al., 1996a,b, 1998). Thermal and epithermal neutron capture rates are treated according to the method of Phillips et al. (2001) and Stone et al. (1998). Scaling to altitude and geographic latitude is based on Stone's (2000) reformulation of Lal (1991). Because of the latitude, i.e. 53°S, changes in geomagnetic field strength are assumed to cause <1% change in ages for the time period studied (Gosse and Phillips, 2001).

Individual exposure ages are shown and discussed with analytical errors only (±1σ) (Tables 3, 4, and 6), and generally without erosion. Ages are also shown with an erosion rate of 1.4 mm/kyr, derived for granite-like

Table 4
Concentration and age data for ^{26}Al measurements

Sample	^{26}Al (10^4 atoms g^{-1})	Age1 No erosion (ka)	Age2 Erosion (ka)	Drift unit
Strait of Magellan lobe				
TF-04-10	100.44±0.68	25.3±2.0	26.1±2.0	Primera Angostura
TF-04-11	103.29±0.96	26.6±2.7	27.5±2.8	Primera Angostura
Bahía Inútil–San Sebastián lobe				
Southeast of Bahía Inútil				
TF-04-05	84.94±1.85	22.0±4.9	22.6±5.0	Bahía Inútil
Between Bahía Inútil and San Sebastián				
TF-04-02	110.98±0.94	25.2±2.4	26.0±2.4	Río Cullen
TF-04-03	90.41±0.90	20.5±2.2	21.0±2.3	Río Cullen

Similar to Table 3 except attenuation length (Brown et al., 1992): 156±12 g cm^{-2}. Procedural blank (10^{-15} with % error): 9.00 (34.4).

rocks at Lago Buenos Aires, mid-latitude Patagonia, ~1000 km to the north (Kaplan et al., 2005). An erosion rate of 1.4 mm/kyr is used to illustrate the effect on apparent cosmogenic ages in southernmost South America if a value from a different setting in semi-arid Patagonia is applied.

4. Results

4.1. ^{10}Be and ^{26}Al

On the oldest, GPG Bella Vista drift, two ^{10}Be ages of 106,000 and 47,400 yr (erosion rate [E]=0 mm/kyr), or 124 and 50 kyr (E=1.4 mm/kyr; Table 3) were obtained. On the younger Cabo Vírgenes Drift, one sample's exposure age is 51 ka (E=0 mm/kyr) or 54 ka (E=1.4 mm/kyr), and on the equivalent Río Cullen Drift (Tables 1 and 3) ten ages range from 50 to 13 ka with a mean and median of 25–26 ka and a standard deviation of ~9 ka (E=0 mm/kyr). A major subset of these Río Cullen ages (8 of 10) cluster between 26 and 19 kyr (1σ). For six of the seven Río Cullen samples near Punta Sinaí, which are all granodiorite erratics, there is no apparent relation between height and age for these boulders (7th column in Table 2), with the exception that the shortest boulder (RC-04-06) is also the youngest. Another notable point for the RC samples is that RC-04-07, which has the longest exposure history (50 ka), is an erratic that is from a different part of the moraine than the other six RC samples, being slightly further inland by ~1 km (Fig. 2C). On the next younger San Sierras de San Sebastián Drift, two samples in close proximity provide considerably different ages of 174 and 21 ka (E=0 mm/kyr) and the higher boulder (close to 5 m, compared to 2.75 m) has the older exposure age. On its correlative around Magellan, the Punta Delgada drift produced an age of 133 ka. The samples on the second to youngest Primera Angostura Drift produce exposure ages from ca. 32 to 22 ka (E=0 mm/kyr), or 33 to 22 ka (E=1.4 mm/kyr). The three samples from the kame terrace southeast of Bahía Inútil (TF-04-04 to 06) are ~18–15 ka.

Within 1σ, all ^{26}Al ages overlap with the respective boulder ^{10}Be ages. Thus, the multi-nuclide approach indicates that (at least) these five boulders have not had a complex history of exposure and prolonged burial (Gosse and Phillips, 2001).

Table 5
Whole rock analyses for ^{36}Cl measurements from southernmost Patagonia–Fuego

Sample	SiO_2 (wt.%)	Al_2O_3 (wt.%)	Fe_2O_3 (wt.%)	MgO (wt.%)	CaO (wt.%)	Na_2O (wt.%)	K_2O (wt.%)	TiO_2 (wt.%)	MnO (wt.%)	P_2O_5 (wt.%)	Cl ppm	Gd ppm	Sm ppm	B ppm
Bahía Inútil Drift/Lagunas Secas Drift?														
TF-04-04	59.38	15.94	6.14	2.07	5.43	3.45	3.295	0.631	0.185	0.499	4.7	5.65	6.51	2.35
TF-04-05	59.13	17.17	5.4	1.83	6.26	3.6	3.181	0.607	0.17	0.544	4.56	5.32	6.05	6.09
Río Cullen Drift														
RC-04-01	58.49	17.56	4.99	1.67	5.83	3.86	3.388	0.598	0.17	0.528	6.53	5.8	6.82	<2.32
RC-04-04f	58.38	17.31	5.44	1.87	5.78	3.92	2.866	0.607	0.19	0.476	31.4	5.67	6.76	<2.32

U and Th not measured, and assumed to be 3±1 and 15±3, respectively.

Table 6
For chlorine analyses, composition of sample dissolved, AMS ratios, and ages

Sample	^{36}Cl	Al_2O_3	TiO_2	Fe_2O_3	MnO	MgO	CaO	Na_2O	K_2O	Age
	(10^4 atoms g^{-1})	(wt.%)	(wt.%)	(wt.%)	(wt.%)	(wt.%)	(wt.%)	(wt.%)	(wt.%)	ka
Bahía Inútil Drift/Lagunas Secas Drift?										
TF-04-04	36.56±1.81	0.34	0.00	0.00	0.00	0.00	0.01	0.02	0.24	54.8±31
TF-04-05	55.04±5.28	1.86	0.00	0.07	0.00	0.03	0.12	0.15	1.21	22.3±2.6
Río Cullen Drift										
RC-04-01	60.71±7.77	1.07	0.00	0.07	0.00	0.00	0.12	0.15	0.50	51.5±7.9
RC-04-04f	30.57±1.15	20.41	0.01	0.16	0.01	0.04	2.70	4.82	5.56	25.2±1.6

The only sample that was 'pure quartz' upon dissolution was TF-04-04; the low chlorine content, and lack of K and Ca production pathways for this sample, led to low concentrations and hence a high uncertainty. Procedural blank: 4.461×10^{-15}.

4.2. ^{36}Cl

Four samples had measurable ^{36}Cl/Cl (Table 6), including the two samples from the kame terrace south of Bahía Inútil and two samples from the Río Cullen Drift near Punta Sinaí. TF-04-05 and RC-04-04f are ~22 ka and 25.2 ka, respectively, in good agreement with the respective ^{10}Be and ^{26}Al ages (Fig. 2). One sample, RC-04-01, produced a ^{36}Cl age of ~50 kyr, whereas the ^{10}Be ages on the same sample are around 20 ka (Tables 3 and 6). The mismatch can't be explained by erosion. The ^{36}Cl errors (~10%) are less than the age discrepancies and there is no solution of time and erosion that allows concordance of the nuclide data (cf., Gosse and Phillips, 2003). Although it is not clear why there is a difference in age between ^{10}Be and ^{36}Cl for this sample (and perhaps TF-04-04), possibly K-feldspar grains were not uniformly distributed among the quartz grains, i.e., there were compositional differences. For ICP analyses, we took a ~1 g aliquot from the sample before dissolution. Even <5% difference in K-feldspar between the aliquot and the rest of the sample that was subsequently dissolved and measured on the AMS would have led to discordant ages.

We attempted to solve for erosion rate and age using ^{10}Be (or ^{26}Al)/^{36}Cl paired analyses (cf., Liu et al., 1994). For TF-04-04, the only pure quartz sample with measurable ^{36}Cl/Cl, the uncertainty is too large, >50%. The other three samples have 'non-overlapping' age/erosion rate solutions, in part because the measured nuclides are produced mainly by spallation, the errors are too large and the samples exposed too recently (cf., Gosse and Phillips, 2003). Nonetheless, for the boulders the multiple nuclide data provide general information on time and erosion. Overall, the ^{36}Cl ages support ^{10}Be—(the most common isotope used here) based inferences for the exposure history (see below). In addition, assuming constant exposure, the ages derived with either nuclide do not change significantly for rates up to ~10 mm/kyr.

5. Discussion

The apparent exposure ages for erratics on old (i.e., pre-LGM) moraines are far less than the limiting ^{40}Ar/^{39}Ar ages provided by interbedded lava flows, and many are younger than minimum ages provided by ^{14}C dates (and supported by AAR analyses) from shelly till in the Strait of Magellan. Albeit, there are only a few boulders found and measured on the pre-LGM drift north of Magellan Strait, but they are all much younger than the ^{40}Ar/^{39}Ar limiting ages. For example, on the 1.1 Myr GPG deposit cosmogenic exposure ages are 47 and 106 ka, and on a deposit ^{40}Ar/^{39}Ar dated >450 ka a ^{10}Be exposure age is 51 ka. In addition, notable age inversions exist in two places. Along the north side of the Strait of Magellan, a boulder age of 133 ka on the Punta Delgada drift is older than the boulder TF-04-08 at 51 ka on the adjacent and older Cabo Vírgenes drift (Fig. 2). A second major age inversion is in northern Tierra del Fuego, where an age of 174 ka (SS-04-01) on San Sebastián Drift is much older than any age on the older Río Cullen drift. These are all minimum ages assuming an erosion rate > 0 mm/kyr. Taken at face value, the 133 and 174 ka ages could indicate the Punta Delgada and San Sebastián drifts were deposited during MIS 6. However, it must be emphasized, particularly in light of processes discussed below, that these are clearly minimum ages, especially for the latter sample, a short ~25 cm high boulder (Fig. 3B). On Tierra del Fuego, glacial drift >400 ka in age contains erratics with relatively short exposure histories, <50 ka, with the important exception of 174 ka. The cosmogenic ages for the San Sebastián and Río Cullen drifts are also far younger than the inferred ages based on U-series and AAR data (Bujalesky et al., 2001) from nearby equivalent marine deposits (Fig. 2D).

Collectively, the cosmogenic data support pre-LGM ages for (at least) the three oldest drift units shown in Table 1. The range and variance of the cosmogenic age distributions are far higher than any LGM deposit studied in middle and southern Patagonia (Kaplan et al., 2004; McCulloch et al., 2005; Douglass et al., 2006), which is outside the high latitude regions where inheritance is a widespread problem (e.g., Briner et al., in press). For example, in three different localities two boulders on the same morainic deposit within 1 km of each other (or even a few 100 m) provide completely different ages, 106 and 50 ka (Bella Vista drift), 50 and 13 ka (Río Cullen drift), and 170 and 21 ka (San Sebastián drift). For the 7 samples on the Río Cullen moraine at Punta Sinaí the standard deviation is ~9 ka, almost the entire age range of the recorded LGM in the nearby Strait of Magellan (McCulloch et al., 2005) and southern Tierra del Fuego (Rabassa et al., 2000). Furthermore, Zreda and Phillips (1995) and Hallet and Putkonen (1994) made a case that on 'old' moraines the oldest age(s) assuming no erosion will be the one closest to the 'true' moraine deposition age, given that the relevant geomorphic processes will almost all lead to minimum ages. On the oldest four drift units in the region (Table 1), the oldest age is greater than the time of LGM (i.e., >25 ka). This assumption is also supported at Lago Buenos Aires ~1000 km to the north (Kaplan et al., 2005).

On the kame terrace southeast of Bahía Inútil all three isotopes provide ages overlapping with LGM time (Fig. 2C), including the TF-04-04 ^{36}Cl age within 1σ. Originally, when sampled in the field, it was assumed that this terrace was just beyond the mapped limit of LGM drift (e.g., see Fig. 2 in Bentley et al., 2005). Based on the analyses presented here, and its position so close to mapped deposits of the last glacial period, we now conclude that the kame terrace was formed during the LGM (Fig. 2A and C).

5.1. Implications for landscape change in Fuego–southernmost Patagonia

For the pre-LGM deposits in Fuego–southernmost Patagonia, we infer that boulder erosion and exhumation from the moraine matrix explains the discrepancy between the cosmogenic ages and the constraining ^{40}Ar/^{39}Ar ages of the interbedded lava flows (and AAR and U-series ages from the Strait of Magellan and Tierra del Fuego). Differences in lithology most likely cannot explain the findings as they are not fundamentally different between samples measured, which are almost all granites or granodiorites with similar composition (e.g., the four boulders shown in Table 5). At Punta Sinaí (and other Río Cullen sites), the erratics are coarse, medium grained, megascopically foliated granodiorites with quartz, plagioclase and K-feldspar (orthoclase) as essential components (D. Acevedo, personal communication). Advanced weathering and erosion of erratics is clearly evident in the form of boulder surface potholes and weathered 'micro-gulleys' 5–10 cm deep, especially on Tierra del Fuego deposits (Fig. 3D, E, and F). As an example, TF-04-01 shown in Fig. 3D provides a young age of 23 ka, yet intense erosion (and exhumation) is obvious on the sides and top of the erratic. Interestingly, the boulders on the Río Cullen drift exhibit relatively more weathering compared to those to the north (e.g., Bella Vista and Cabo Vírgenes drifts) and in general provide younger ages (Fig. 2), despite a roughly similar lithology (granite or granodiorite). There appears to be no obvious general relation between boulder height and age, except for the two San Sebastián erratics measured. On the Río Cullen drift near Punta Sinaí, the only distinct difference for the boulder with the oldest and statistically higher age is that it is from a different part of the moraine, being further inland by ~1 km, than the other 6 samples.

There is a non-unique combination of erosion, exhumation and reburial that could have produced the apparent ages, all operating in an episodic or gradual manner. Any burial was brief (less than the last glacial cycle) as indicated by the ^{26}Al/^{10}Be (and ^{36}Cl) ratios. For the sake of discussion, if no exhumation and a steadily eroding surface are assumed, then boulder maximum 'model' erosion rates can be estimated for the oldest apparent samples and by assuming ages >400 ka for the Cabo Vírgenes Drift, 1.1 Myr for the Bella Vista drift, and >400 ka for the San Sebastián and Río Cullen Drifts (Bujalesky et al., 2001). It is emphasized that these are only 'apparent' rates and they are presented to infer geomorphic processes that may have caused given isotope concentrations in southernmost South America. This simple exercise produces erosion rates for boulder material of >5 and 11 mm/kyr (Bella Vista drift), >3 mm/kyr for San Sebastián Drift, and >11 mm/kyr for the Cabo Vírgenes Drift (Fig. 4A). Almost identical erosion rates are calculated assuming that isotope concentrations are in secular equilibrium (Lal, 1991).

Available evidence indicates that, in general, boulders erode slower than their surrounding landscape, thus the erosion rates presented above may be less than that for the moraine matrix, provided there is no desert pavement or matrix cement (Granger et al., 2001). For the sake of discussion, if the apparent ages are due entirely to exhumation (i.e., no erosion), then a stripping of up to at

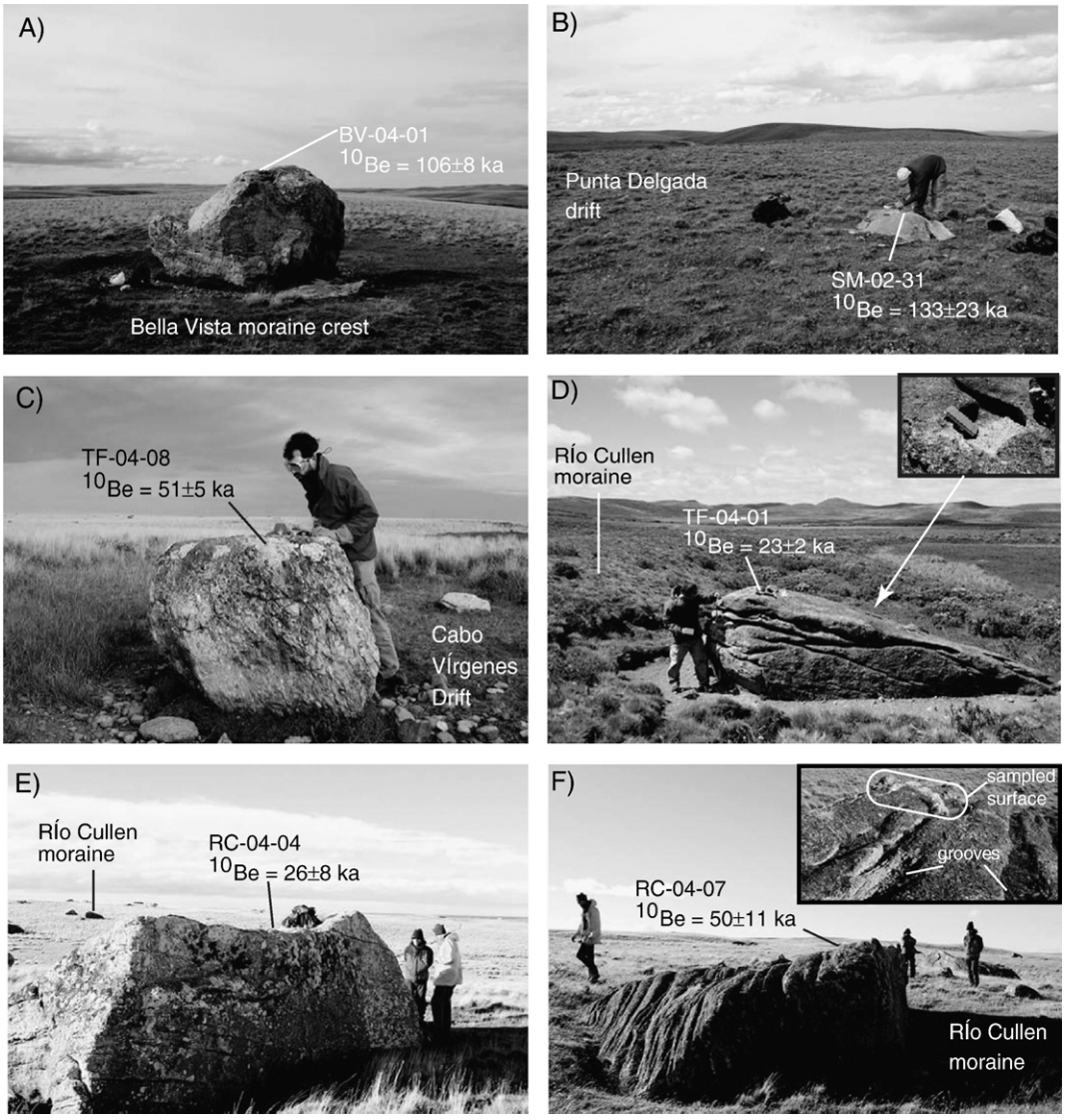

Fig. 3. Pictures of samples in Fuego–southernmost Patagonia. A. Moraine crest on the Bella Vista drift, the local equivalent of the Greatest Patagonian Glaciation (GPG), dated to 1.1 Myr (Meglioli, 1992; Singer et al., 2004), and sample BV-04-01 with age. B. Broad flat Punta Delgada drift moraine crest with sample SM-02-31. C. Broad flat Cabo Vírgenes drift in background, along with sample TF-04-08. D. Sample TF-04-01 on Río Cullen moraine crest. Note deep weathering grooves of granodiorite sample. Also shown in inset is pothole with field notebook for scale. E. Sample RC-04-04 on the Río Cullen moraine near Punta Sinaí. Other large erratics are shown in background. F. Sample RC-04-07 with inset showing deep weathering grooves on top surface near sampled location.

least ~2–3 m (i.e., amount needed to have the 'clock' at ~0 yr prior to exposure) of moraine matrix during the last glacial cycle could explain the nuclide concentrations (except for SS-06-01), assuming the boulders had no inherited cosmogenic nuclides prior to being exposed at the moraine surface; considering erosion decreases the amount of stripping (e.g., <2–3 m) needed to explain the apparent ages. Also, the boulders could have had a complex history of exposure and burial (e.g., due to loess) since moraine formation, which has kept isotope concentrations relatively low. For sample SS-06-01, given its height at ~5 m off the ground, a combination of erosion and exhumation seems likely.

A key point is that long-term erosion and/or exhumation rates must be low enough that the old deposits still exist, and in some areas with original morphologic features. The $^{40}Ar/^{39}Ar$ dated Bella Vista and Cabo Vírgenes drifts, and correlatives such as the Río Cullen

drift, still contain (subdued) moraine crests and ice molded landforms (Meglioli, 1992; Rabassa et al., 2000; Coronato et al., 2004a,b; Ercolano et al., 2004). In addition, meltwater systems linked to the original glaciation (or deglaciation) that deposited the given moraine drift, including the Cabo Vírgenes and Bella Vista units (which are overlain by the dated lava flows), are still clearly visible and easily mapped (see Fig. 2). As shown in Fig. 2, subsequent glaciations are 'nested' within each other and the younger ones are at inner and/or lower positions in the landscape. Thus, it is unlikely that landforms on the surface of the drift have been reworked or reburied by younger, major glaciations (e.g., forming meltwater channels fundamentally different in age).

Given that the 'old' glacial deposits, with original characteristics including meltwater channels, contain erratics with relatively low cosmogenic nuclide concentrations, an explanation is that short but intense periods of erosion, exhumation (e.g., loess removal) or reburial during glaciations or interglaciations must cause ^{10}Be, ^{26}Al and ^{36}Cl ages to provide comparatively recent minimum ages. Boulder exposure ages for any given dated moraine are up to an order of magnitude less than the limiting ^{40}Ar/^{39}Ar ages. Taken at face value, these nuclide concentrations and the ^{40}Ar/^{39}Ar data imply erosion of >10 m since moraine formation (or exhumation ~10–20 m). If such erosion or exhumation rates have been constant, we infer that moraine crests, meltwater channels, and other features should not be expected, at least not without repeated reburial (e.g., by loess). Thus, over the history of the moraine, boulder erosion or exhumation rates could not have been constant.

The cosmogenic data may indicate that boulders located near Punta Sinaí, in general, appear to be eroding more quickly (or have been exhumed more recently) than those farther to the north on the Bella Vista and Punta Deglada Drifts (Figs. 2 and 4), except perhaps for SS-04-01. This finding is consistent with surface erosional features on boulders (Fig. 3), as Tierra del Fuego erratics typically contain deep relief (>5 cm)

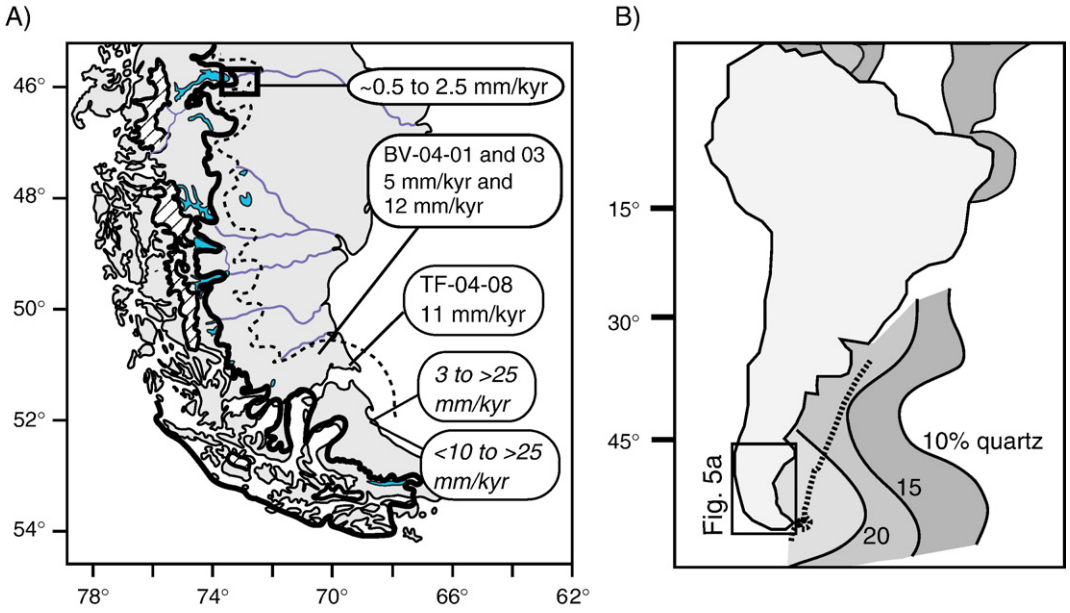

Fig. 4. Comparison of terrestrial and marine information concerning southern South American landscape change. A) 'Apparent' maximum boulder erosion rates assuming no exhumation, steady exposure, and the given nuclide concentrations. It is emphasized that these 'apparent' rates are shown for the sake of discussion to illustrate different geomorphic processes operating in southernmost South America. For Lago Buenos Aires, rates derived using nuclide concentrations on moraines >760 ka (Kaplan et al., 2005). For southernmost Patagonia, rates estimated using nuclide concentrations on deposits constrained in age with dated interbedded lava flows (Fig. 2A). These rates are similar to those estimated assuming isotope concentrations have reached a secular equilibrium where production equals removal due to decay and erosion (Lal, 1991). Also shown are rates for the measured boulders on Sierras de San Sebastián and Río Cullen moraines on Tierra del Fuego, assuming ages of >400 ka based on morphostratigraphically related marine deposits (see text). For the Río Cullen moraine, the lower rate shown (i.e., <10 mm/kyr) is based on assuming an age of >400 ka for RC-04-07, and the higher rate (>25 mm/kyr) is based or assuming this age (or secular equilibrium) for the other Río Cullen samples. The data also can be used to show higher rates of possible exhumation southward (see text). B) From Kolla et al. (1979). Distribution of weight percent quartz (carbonate free) in sediments of the last glacial times (i.e., last glacial maximum of CLIMAP). The authors also noted that adjacent to southernmost Patagonia there was no significant difference between the percent quartz of the last glaciation and Holocene sediments. Also shown is former sea level (dotted line) and approximate outline of area in Fig. 4A. In addition, note that at present the average annual position of the westerlies lies around 50°S.

and potholes, indicating advanced stages of erosion, which were not observed on southern Patagonian erratics (Fig. 3). A possibility is that during the LGM and pre-LGM glaciations, Río Cullen boulders were eroded more rapidly by frost action. Periglacial or permafrost conditions existed at the present Atlantic coast during the LGM, as demonstrated by the nearby presence of ice-wedges in the area around the town of Río Grande (Coronato et al., 2004c; Perez Alberti et al., 2005). Also, several marine transgressions could have facilitated salt weathering and high erosion rates at Puna Sinaí, which is near the coast. Perhaps, the climate has been harsher (i.e., colder or wetter) on Tierra del Fuego than in Southernmost Patagonia, due to the slightly more southerly location and higher humidity, (Fig. 4), and close proximity of the Darwin Cordillera ice mass, the largest part of the southernmost Patagonia ice sheet at the LGM. It should be noted that for northern Tierra del Fuego, in general, the landscape development has been different from that of the 'Patagonian tablelands' due to regional climate and marine influence (Clapperton, 1993; Coronato et al., in press).

5.2. Implications for landscape change in Southern Patagonia

Exposure histories of pre-LGM boulders in southernmost Patagonia–Fuego are quite unlike those in the middle latitudes of Patagonia. In semi-arid mid-latitude Patagonia at Lago Buenos Aires (LBA) (Fig. 1), moraines that are at least two and perhaps three glacial cycles old can be constrained in age with cosmogenic nuclide concentrations in erratics (Kaplan et al., 2005). 'Apparent' rates of boulder erosion or exhumation (or reburial) at LBA were estimated by measuring the concentrations of ^{10}Be and ^{26}Al in glacial erratics on the oldest moraines, which are constrained in age independently with ^{40}Ar/^{39}Ar data to between 760 ka and 1100 ka (Singer et al., 2004; Kaplan et al., 2005). The LBA 'apparent' rates are almost all <2.5 mm/kyr, with a variability of ~1 mm/kyr, much less than 'apparent model rates' anywhere in this investigation on Fuego–southernmost Patagonia. Most recent ^{36}Cl/^{10}Be pairing at LBA indicates rates (Douglass, 2005) even slightly lower than those presented in Kaplan et al. (2005). For comparison, boulder surface erosional features such as potholes, relief >5 cm, and deep rills evident on Tierra del Fuego boulders (Fig. 3), are rare at LBA where mainly evidence of wind ventifaction is commonly observed (e.g., see Fig. 3 in Kaplan et al., 2005). Applying erosion rates derived at LBA, ~1.4 mm/kyr, to boulder ages in Fuego–southern Patagonia (Table 3) does not increase the ages even close to the ^{40}Ar/^{39}Ar minimum age constraints for these moraines. Given the different findings for pre-LGM moraines at LBA compared with the area of this study, the erosion rates derived for the former obviously are not applicable (or comparable?) to the latter, in part because it is unclear how the nuclide concentrations were produced in the different geomorphic settings.

At the very least, the evidence suggests that geomorphic processes in Fuego–southernmost Patagonia are quite different compared to that in the LBA area and the middle latitudes (Fig. 4). Important differences between Fuego–southernmost South America and LBA could include the following.

1) Temperatures have been lower or precipitation higher southward, especially during glacial times. Presently, the LBA climate is classified (Fig. 5) as arid (aridity index=0.2), the area around Bella Vista as cold sub-arid (aridity index=0.5), and around Punta Sinaí as cold, sub-humid and oceanic (aridity index=0.75) (Aridity index=mean annual rainfall/potential evapotranspiration [UNESCO, 1977]). Currently, Tierra del Fuego is only 3–5° north of the Antarctic Frontal Zone, which may have maintained a more northerly position during the LGM (Ackert et al., 2003; Sugden, 2005; Kaplan et al., in preparation). In addition, compared to at LBA and the mid-latitudes, the Southern Hemisphere westerlies transport more humid air to Tierra del Fuego, and especially near Punta Sinaí at the coast, for most of the year the temperature range is less and soils are more humid (i.e., more moisture in the air) (Fig. 5; Coronato et al., in press). An observed record of LGM permafrost features on Tierra del Fuego but not at LBA may attest to colder more humid conditions further south during glacial times (Clapperton, 1993; Coronato et al., 2004c; Perez Alberti et al., 2005).
2) Wind erosion has been more intense in Fuego–southernmost Patagonia, especially during the LGM when the sea was ~250 km distant and a broad continental shelf was exposed (Fig. 4). Presently, southernmost South America lies in the core of the westerlies (Taljaard et al., 1969). High aeolian dust in southern Patagonia during 'glacial times' is well-documented by local terrestrial (Rabassa et al., 2000), nearby marine (Kolla et al., 1979; Fig. 4B) and Antarctic ice core studies (Delmonte et al., 2004). Although the exact source area of dust in Patagonia is still debated (Delmonte et al., 2004), possibly, more aeolian material exists or there are stronger winds during glacial maxima (i.e., causing more intense wind abrasion and erosion) towards southernmost South America.

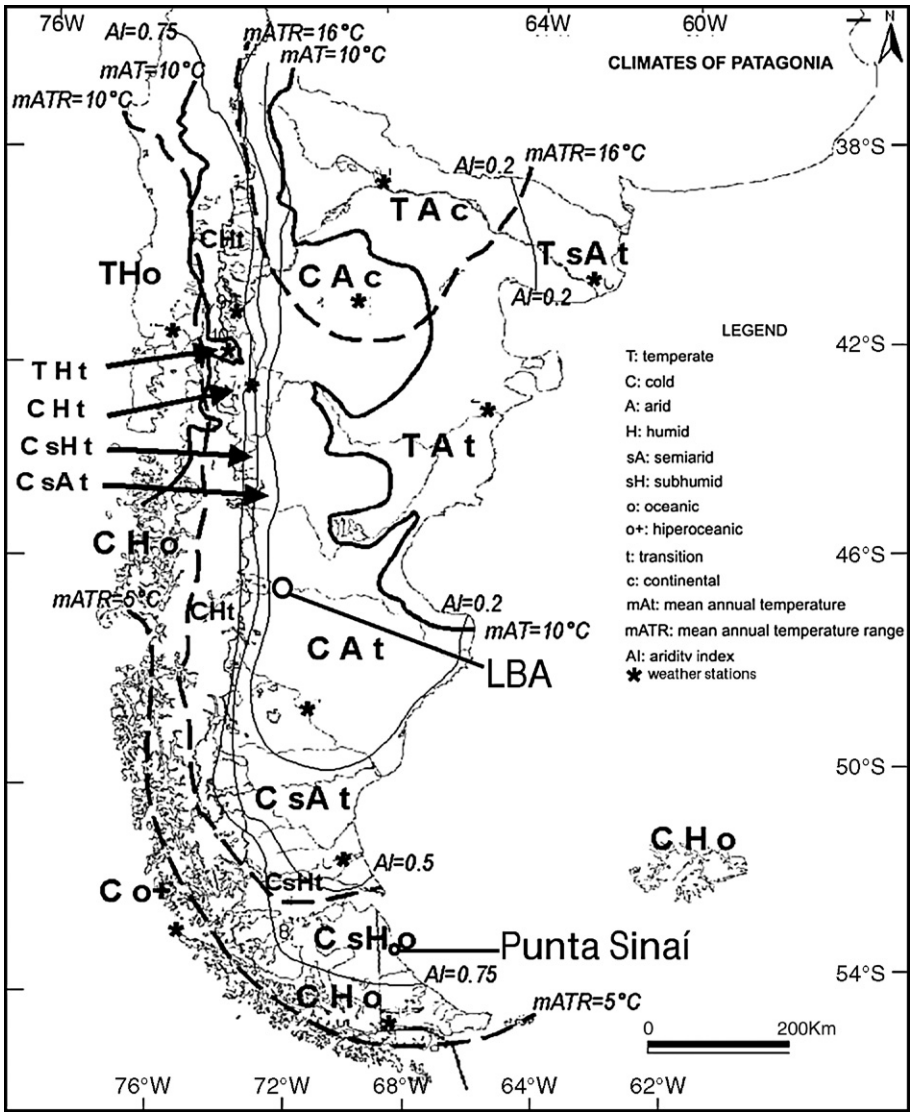

Fig. 5. By F. Coronato in Coronato et al. (in press). Temperature data and climate 'zones' including aridity index (AI), which is defined as (UNESCO, 1977): AI < 0.2 = arid; 0.2 < AI < 0.5 = semi-arid; 0.5 < AI < 0.75 = sub-humid; AI > 0.75 = humid. Note differences in climate between the Lago Buenos Aires area and Fuego–southern Patagonia.

3) Proximity to the sea during interglacial periods has led to differences in weathering (i.e., salt weathering). Throughout much of the last glacial cycle sea level was far from the present coastline on the broad Argentine continental shelf (Fig. 4B), e.g., during the LGM the coastline was >250 km away. In contrast, (at least) since MIS 11, during interglacial periods, the sea has been close to its present position at Punta Sinaí (Bujalesky et al., 2001). The oldest exposure age near Punta Sinaí is also farthest from the present coastline.

In summary, more intense aeolian abrasion, colder or more humid conditions, or proximity to the sea could explain the observation of 'apparent' higher boulder and moraine erosion rates towards the southern tip of South America.

6. Summary and conclusions

Cosmogenic nuclide data in southernmost South America indicate that glacial erratics have much shorter exposure durations than the ages of the landforms they sit upon. In southern Patagonia and on northern Tierra del Fuego, the range and variability of the cosmogenic ages are in agreement with the moraines being old, i.e., pre-last glacial maximum (LGM) or older than MIS 2

(Mercer, 1983; Meglioli, 1992; Rabassa et al., 2000; Coronato et al., 2004a,b; Singer et al., 2004). Geomorphic processes are causing profound differences in exposure ages on pre-LGM deposits, even within 1 km. These processes do not seem to be as pervasive on LGM deposits to the west, within the Strait of Magellan and around Bahía Inútil, where interestingly cosmogenic dating has excellent potential for elucidating the chronology of LGM glacial deposits, as evident by good agreement with a ^{14}C-based chronology (McCulloch et al., 2005; Kaplan et al., in preparation).

An explanation that accommodates various lines of evidence is that fast episodic erosion rates occurred only during peak glacial times, perhaps aided by periglacial processes (Coronato et al., 2004c; Perez Alberti et al., 2005). Such a history takes into account observations of original morphologic features (e.g., Ercolano et al., 2004) on drift up to 1 Myr, or at least >450 ka, and the relative 'youthfulness' of boulder exposure data. This could also explain why many of the ages on the Punta Delgada and Río Cullen deposits are in the 30–13 ka range (i.e., the last glacial period). The nuclide concentration data indicate that, essentially, most of the surface boulders have total exposure histories of about 100 ka or less, which is the approximate length of the last glacial cycle. The evidence may imply that the erratics are eroding relatively quickly or they all have been exhumed from the moraine matrix within the last glacial cycle, whereas the geomorphic processes that limit the utility of the cosmogenic chronometers on pre-LGM deposits have not had such a pervasive effect over the last ~17 ka.

The age distributions thus indicate that cosmogenic nuclide dating cannot be used reliably as a chronometer on glacial deposits older than the LGM in Fuego–southernmost Patagonia. For comparison, in the middle latitudes of Patagonia at Lago Buenos Aires, cosmogenic dating holds excellent potential to date pre-LGM moraines (Kaplan et al., 2005; Douglass et al., 2006). Thus, appreciation of present and past climate regimes can serve as a useful guide to the limit of the probable utility of the technique on old glacial surfaces.

The 'short' exposure history of boulders on old pre-LGM moraines in Fuego–southernmost Patagonia, compared to the findings from Lago Buenos Aires in central Patagonia, leads us to hypothesize that towards the southern tip of South America geomorphic processes (e.g., boulder erosion or exhumation rates) have been operating differently over at least the last few glacial cycles. Higher rates of landscape change between middle and high latitude South America is compared with offshore data (Fig. 4B). Although there was a limited amount of data, the work of Kolla et al. (1979) did show increased percent quartz by weight of sediment, i.e., increased aeolian input, in the past (and present) towards the south in the adjacent southwest Atlantic Ocean. The marine data may reflect higher production and thus availability of quartz-bearing sediments due to glacial or non-glacial erosion. The terrestrial, and perhaps marine, evidence may suggest that towards southern South America overall landscape denudation has been faster during the Quaternary Period.

Acknowledgments

We thank Charlie Mann at Estancia Sara (where Punta Sinaí is located), Steven Binnie, Rob Ellam, Dodie James, Willie Gibson, Anthony Newton and Scott Dreher. Special thanks to John Stone and Robert Finkel for ^{36}Cl instruction, data and analyses. Comments from Steve Binnie, David Fink, and reviews by Florian Kober and an anonymous reviewer greatly clarified and strengthened the manuscript. This research was supported by a Royal Society of London Postdoctoral Fellowship (Kaplan) a NERC Small Grant NER/B/S/2003/00286 (Hulton and Kaplan), and SECYT-CONICET (Coronato and Rabassa).

References

Ackert, R.P., Singer, B.S., Guillou, H., Kaplan, M.R., Kurz, M.D., 2003. Long-term cosmogenic 3He production rates from ^{40}Ar/^{39}Ar and K–Ar dated Patagonian lava flows at 47°S. Earth Planet. Sci. Lett. 210, 119–136.

Bentley, M.J., Sugden, D.E., Hulton, N.R.J., McCulloch, R.D., 2005. The landforms and pattern of deglaciation in the Strait of Magellan and Bahía Inútil, Southernmost South America. Geogr. Ann. 87A, 313–333.

Bierman, P.R., Caffee, M.W., Davis, P.T., Marsella, K., Pavich, M., Colgan, P., Mickelson, D., 2002. Rates and timing of earth surface processes from in situ-produced cosmogenic Be-10. In: Grew, E.S. (Ed.), Beryllium: mineralogy, petrology, and geochemistry. Series: Reviews in mineralogy and geochemistry, vol. 50. Mineralogical Society of America, Washington D.C.

Briner, J.P., Gosse, J.C., Bierman, P.R., in press. Applications of cosmogenic nuclides to Laurentide Ice Sheet history and dynamics. In: Siame, L. (Ed.), Applications of cosmogenic nuclides to the study of Earth surface processes: the practice and the potential. Geological Society of America.

Brown, E.T., Brook, E.J., Raisbeck, G.M., Yiou, F., Kurz, M.D., 1992. Effective attenuation of cosmic rays producing ^{10}Be and ^{26}Al in Quartz: implications for exposure dating. Geophys. Res. Lett. 19, 369–372.

Bujalesky, G., Coronato, A., Isla, F., 2001. Ambientes glacifluviales y litorales Cuaternarios de la región del Río Chico, Tierra del Fuego, Argentina. Rev. Asoc. Geol. Argent. 56, 73–90.

Caldenius, C.G., 1932. Las glaciaciones Cuaternarias en la Patagonia and Tierra del Fuego. Geogr. Ann. 14, 1–164.

Clapperton, C.M., 1993. Quaternary Geology and Geomorphology of South America. Elsevier, Amsterdam.

Clapperton, C.M., Sugden, D.E., Kauffman, D., McCulloch, R.D., 1995. The last glaciation in central Magellan Strait, southernmost Chile. Quat. Res. 44, 133–148.

Codignoto, J., Malumian, N., 1981. Geología de la Región al N del paralelo 54°L.S. de la Isla Grande de Tierra del Fuego. Rev. Asoc. Geol. Argent. 36, 44–88.

Coronato, A., Roig, C., Rabassa, J., Meglioli, A., 1999. Erratic boulder field of Pre-Illinoian age at Punta Sinaí, Tierra del Fuego, Southernmost South America. XV INQUA Congress, Durban, South Africa, pp. 47–48.

Coronato, A., Martinez, O., Rabassa, J., 2004a. Pleistocene Glaciations in Argentine Patagonia, South America. In: Ehlers, J., Gibbard, P. (Eds.), Quaternary Glaciations – Extent and Chronolgy. Part III: South America, Asia, Africa Australia and Antarctica. Quaternary Book Series. Elsevier Publishers, Amsterdam, pp. 49–67.

Coronato, A., Meglioli, A., Rabassa, J., 2004b. Glaciations in the Magellan Straits and Tierra del Fuego, Southernmost South America. In: Ehlers, J., Gibbard, P. (Eds.), Quaternary Glaciations– Extent and Chronology. Part III. Quaternary Book Series. Elsevier Publishers, pp. 45–48.

Coronato, A., Bujalesky, G., Perez Alberti, A., Rabassa, J., 2004c. Evidencias criogénicas fósiles en depósitos marinos interglaciarios de Tierra del Fuego, Argentina. X Reunión Argentina de Sedimentología, Resúmenes, San Luis, Argentina, pp. 48–49.

Coronato, A., Coronato, F., Mazzoni, E., Vázquez, M., in press. The physical geography of Patagonia and Tierra del Fuego. In: Rabassa, J. (Ed.), Late Cenozoic of Patagonia and Tierra del Fuego Development in Earth Surface Processes Series, Elsevier.

Delmonte, B., Basile-Doelsch, I., Petit, J.-R., Maggi, V., Revel-Rolland, M., Michard, A., Jagoutz, E., Grousset, F., 2004. Comparing the Epica and Vostok dust records during the last 220,000 years: stratigraphical correlation and provenance in glacial periods. Earth-Sci. Rev. 66, 63–87.

Douglass, D.C., 2005. Glacial chronology, soil development, and paleoclimate reconstructions for mid-latitude South America, 1 Ma to present. PhD dissertation, University of Wisconsin, Madison.

Douglass, D.C., Singer, B.S., Kaplan, M.R., Mickelson, D.M., Caffee, M.W., 2006. Cosmogenic nuclide surface exposure dating of boulders on last-glacial and late-glacial moraines, Lago Buenos Aires, Argentina: interpretive strategies and paleoclimate implications. Quaternary Geochronology 1, 43–58.

Ercolano, B., Mazzoni, E., Vázquez, M., Rabassa, J., 2004. Drumlins y formas drumlinoides del Pleistoceno Inferior en Patagonia Austral, Provincia de Santa Cruz. Rev. Asoc. Geol. Argent. 59, 771–777.

Gosse, J.C., Phillips, F.M., 2001. Terrestrial in situ cosmogenic nuclides: theory and application. Quat. Sci. Rev. 20, 1475–1560.

Gosse, J.C., Stone, J.O., 2001. Terrestrial cosmogenic nuclide methods passing milestones toward paleo-altimetry. EOS 82, 82, 86, 89.

Granger, D.E., Riebe, C.S., Kirchner, J.W., Finkel, R.C., 2001. Modulation of erosion on steep granitic slopes by boulder armoring, as revealed by cosmogenic ^{26}Al and ^{10}Be. Earth Planet. Sci. Lett. 186, 269–281.

Hallet, B., Putkonen, J.K., 1994. Surface dating of dynamic landforms. Young boulders on aging moraines. Science 265, 937–940.

Ivy-Ochs, S., 1996. The dating of rock surfaces using in situ produced ^{10}Be, ^{26}Al, and ^{36}Cl, with examples from Antarctica and the Swiss Alps. Ph. D. Thesis, Swiss Federal Institute of Technology Zurich, Zurich.

Kaplan, M.R., Ackert, R.P., Singer, B.S., Douglass, D.C., Kurz, M.D., 2004. Cosmogenic nuclide chronology of millennial-scale glacial advances during O-isotope Stage 2 in Patagonia. Geol. Soc. Amer. Bull. 116, 308–321.

Kaplan, M.R., Douglass, D.C., Singer, B.S., Ackert, R.P., Caffee, M.W., 2005. Cosmogenic nuclide chronology of pre-last glaciation maximum moraines at Lago Buenos Aires, 46°S. Argentina. Quat. Res. 63, 301–315.

Kaplan, M.R., Fogwill, C.J., Sugden, D.E., Hulton, N.R.J., Kubik, P.W., Freeman, S.P.H.T., in preparation. Southern Patagonian and Southern Ocean Climate During the Last Glaciation.

Kolla, V., Biscaye, P.E., Hanley, A.F., 1979. Distribution of quartz in Late Quaternary Atlantic Sediments in relation to climate. Quat. Res. 11, 261–277.

Kubik, P., Ivy-Ochs, W., Masarik, S., Frank, J., Schlüchter, M., 1998. ^{10}Be and ^{26}Al production rates deduced from an instantaneous event within the dendron–calibration curve, the landslide of Köfels, Ötz Valley Austria. Earth Planet. Sci. Lett. 161, 231–241.

Lal, D., 1991. Cosmic ray labeling of erosion surfaces: in-situ nuclide production rates and erosion models. Earth Planet. Sci. Lett. 104, 424–439.

Liu, B., Phillips, F.M., Fabryka-Martin, J.T., Fowler, M.M., Stone, W.D., 1994. Cosmogenic ^{36}Cl accumulation in unstable landforms. 1. Effects of the thermal neutron distribution. Water Resour. Res. 30, 3115–3125.

McCulloch, R.D., Fogwill, C.J., Sugden, D.E., Bentley, M.J., Kubik, P.W., 2005. Chronology of the last glaciation in the central Strait of Magellan and Bahía Inútil, southernmost South America. Geogr. Ann. 87A, 289–312.

Meglioli, A., 1992. Glacial geology and chronology of southernmost Patagonia and Tierra del Fuego, Argentina and Chile. Ph.D. thesis. Lehigh University, USA.

Mercer, J.H., 1983. Cenozoic glaciation in the southern hemisphere. Annu. Rev. Earth Planet. Sci. 11, 99–132.

Perez Alberti, A., Valcarcel Díaz, M., Carrera Gómez, P., Coronato, A., Rabassa, J., 2005. Late Pleistocene ice-wedge casts from Tierra del Fuego, Argentina. Terra Nostra, 2nd European Conference on Permaforst. Programme and Abstracts, EUCOP IIAWI. Postdam, Germany, pp. 19–20.

Phillips, F.M., Stone, W.D., Fabryka-Martin, J.T., 2001. An improved approach to calculating low-energy cosmic-ray neutron fluxes near the land–atmosphere interface. Chem. Geol. 175, 689–701.

Porter, S.C., 1990. Character and ages of Pleistocene drifts in a transect across the Strait of Magellan. Quat. South Am. Antarct. Penins. 7, 35–49.

Putkonen, J., O'Neal, M.A., 2006. Quaternary degradation of unconsolidated landforms in the western North America. Geomorphology 75, 408–419.

Rabassa, J., Coronato, A., Bujalesky, G., Roig, C., Salemme, M., Meglioli, A., Heuser, C., Gordillo, S., Borromei, A., Quatrocchio, M.J., 2000. Quaternary of Tierra del Fuego, Southernmost South America: an updated review. Quat. Int. 68, 217–240.

Rabassa, J., Coronato, A., Salemme, M., 2005. Chronology of the Late Cenozoic Patagonian Glaciations and their correlation with biostratigraphic units of the Pampean Region (Argentina). J. South Am. Earth Sci. 20, 81–103.

Rutter, N., Schnack, E., Del Rio, J., Fasano, J., Isla, F., Radke, U., 1989. Correlation and dating of Quaternary littoral ones along the Patagonian coast, Argentina. Quat. Sci. Rev. 8, 213–234.

Singer, B.S., Thompson, R.A., Dungan, M.A., Feeley, T.C., Nelson, S.T., Pickens, J.C., Brown, L.L., Wulff, A.W., Davidson, J.P., Metzger, J., 1997. Volcanism and erosion during the past 930 thousand years at the Tatara–San Pedro complex, Chilean Andes. Geol. Soc. Amer. Bull. 109, 127–142.

Singer, B.S., Ackert, R.P., Guillou, H., 2004. ^{40}Ar/^{39}Ar and K–Ar chronology of Pleistocene glaciations in Patagonia. Geol. Soc. Amer. Bull. 116, 434–450.

Stone, J.O., 2000. Air pressure and cosmogenic isotope production. J. Geophys. Res. 105, 23753–23759.

Stone, J.O., Allan, G.L., Fifield, L.K., Cresswell, R.G., 1996a. Cosmogenic chlorine-36 from calcium spallation. Geochim. Cosmochim. Acta 60, 679–692.

Stone, J.O., Evans, J.M., Fifield, L.K., Cresswell, R.G., Allan, G.L., 1996b. Cosmogenic Cl-36 production rates from calcium and potassium. Radiocarbon 38, 170–171.

Stone, J.O., Evans, J.M., Fifield, L.K., Allan, G.L., Cresswell, R.G., 1998. Cosmogenic chlorine-36 production in calcite by muons. Geochim. Cosmochim. Acta 62, 433–454.

Sugden, D.E., 2005. Late-glacial glacier events in southernmost South America and their global significance. Geogr. Ann. 87A, 1–408.

Taljaard, J.J., van Loon, H., Cructcher, H.L., Jenne, R.L., 1969. Climate of the upper air: Southern Hemisphere. Vol 1, temperatures, dew points, and heights at selected levels NAVAIR 50-1C-55, chief naval operations, Washington D.C.

Ton-That, T., Singer, B., Mörner, N., Rabassa, J., 1999. Datación de lavas basálticas por $^{40}Ar/^{39}Ar$ y geología glacial de la región del Lago Buenos Aires. Rev. Asoc. Geol. Argent. 54, 333–352.

UNESCO, 1977. Carte de la répartition mondiale des régions arides. Notes techniques du MAB, n°7. Paris.

Zreda, M.G., Phillips, F.M., 1995. Insights into alpine moraine development from cosmogenic ^{36}Cl buildup dating. Geomorphology 14, 149–156.